



Ionized oxygen around starforming galaxies

E. O. Vasiliev, M. V. Ryabova, and Yu. A. Shchekinov

Institute of Physics, Department of Physics, Southern Federal University, Stachki Ave. 194,
Rostov-on-Don, 344090 Russia, e-mail: eugstar@mail.ru

Abstract. We consider the evolution of metal-enriched gas exposed to a superposition of time-dependent radiation field of a nearby starburst galaxy and nearly invariant (on timescales 100 Myr) extragalactic ionization background. We study the evolution of ionic species depending on the galactic mass and star formation rate, and derive conditions for the highly ionized oxygen, O VI, to appear in extended galactic haloes in absorption or emission spectra. We have found that the maximum O VI fraction can reach $\sim 0.4 - 0.6$ under the action of both ionizing radiation field, which is typical in haloes of starforming galaxies, and the extragalactic background, the fraction remains high in a wide temperature range. We study the dependence of the O VI ion fraction on gas density and found that for the typical density of the circumgalactic gas, $n \sim (0.5 - 2) \times 10^{-4} \text{ cm}^{-3}$ the O VI fraction is higher than ~ 0.1 at distances $r \sim 50 - 120 \text{ kpc}$. We have shown that the O VI fraction is high enough that *even* for $\sim 0.1Z_{\odot}$ metallicity we can explain large O VI column densities ($\log[N(\text{OVI}), \text{cm}^{-2}] \sim 14.5 - 15.3$) observed in the haloes of starforming galaxies by Tumlinson et al. (2011). Thus, the requirements to the sources of oxygen supply into the extended haloes become reasonably conservative.

Key words. galaxies: evolution – haloes – starburst – theory – diffuse radiation – intergalactic medium – quasars: general – absorption lines – physical data and processes: atomic processes

1. Introduction

High O VI column densities observed in the haloes of starforming galaxies at $z \sim 0.1 - 0.4$ by Tumlinson et al. (2011) allow to conclude that huge (up to 150 kpc) haloes contains a substantial mass of metals and gas, perhaps far exceeding the reservoirs of gas in the galaxies themselves (Tumlinson et al. 2011). O VI is a fragile ionic state in the sense that under standard assumptions of thermal ionization its fraction never exceeds ~ 0.2 and such a high value is reached only in a narrow temperature range (e.g. Ferland et al. 1998; Gnat & Sternberg 2007). As a result, conservative estimates of

circumgalactic gaseous mass force to assume solar metallicity for a gas in the extending up to 150 kpc haloes of star-forming galaxies. Here we study the evolution of ionic composition of a gas in the halos of star-forming galaxies taking into account starformation history.

2. The model and initial conditions

Our model includes the following ingredients

- the ionization and thermal evolution of gas: nonequilibrium (time-dependent) ionization kinetics for H, He, C, N, O, Ne, Mg, Si, Fe and self-consistent cooling and heat-

- ing rates, in total 96 ordinary differential equations (see details in Vasiliev 2011);
- the extragalactic spectrum: (Haardt & Madau 2001) spectra for 49 redshifts;
- the UV galactic spectrum was calculated using the PEGASE code (Fioc & Rocca-Volmerange 1997);
- the X-ray galactic spectrum calculated using the “ $L_X - SFR$ ” relation (Gilfanov et al. 2004);
- a power-law starformation rate (SFR): $SFR(t) = M_g^{p_1} / p_2$, where M_g is the galactic gaseous mass and $p_1 = 2$, the initial gaseous mass is $M_g^i = 10^{11} M_\odot$;
- the galactic halo gas exposed to the cumulative galactic and extragalactic ionizing radiation, the galactic part of the spectrum being attenuated by the underlying neutral gas: $\tau_\nu = \sigma_\nu^{\text{HI}} N_{\text{HI}} + \sigma_\nu^{\text{HeI}} N_{\text{HeI}}$, where $N_{\text{HI}} = 10^{20} \text{ cm}^{-2}$, $N_{\text{HeI}} = 10^{19} \text{ cm}^{-2}$ are assumed.

We assume that the halos of massive star-forming galaxies are similar to that of the Milky Way. According to the recent simulations of the Milky Way halo the number density of a gas is found to range within $\sim (0.5 - 2) \times 10^{-4} \text{ cm}^{-3}$ at distances $\sim 50 - 300 \text{ kpc}$ (Feldmann et al. 2013). The observational estimates of the circumgalactic gas density give $\sim (1 - 3) \times 10^{-4} \text{ cm}^{-3}$ at $r \sim 40 - 150 \text{ kpc}$ (e.g., Stanimirović et al. 2002; Anderson & Bregman 2010). So that for the number density of the circumgalactic gas we adopt $n = (0.5 - 4) \times 10^{-4} \text{ cm}^{-3}$ in our calculations.

We start our calculation at $z = 2$ (the look-back time is around 10 Gyrs). At first, this timescale is about cooling time for hot gas with $T \sim 10^6 \text{ K}$ and $\sim (0.5 - 2) \times 10^{-4} \text{ cm}^{-3}$ (Feldmann et al. 2013). At second, the last major merging for the Milky Way type galaxies is thought to be earlier than $z \sim 2$ (e.g., Hammer et al. 2007).

The initial ionic composition and temperature are set to the ones corresponding to photoequilibrium in a gas exposed to the extragalactic Haardt & Madau spectrum at $z = 2$. This radiation background is sufficiently high to force such low density gas into photoequilibrium (Vasiliev 2011).

We study the evolution of a gas with metallicity ranged from 10^{-2} to $0.1 Z_\odot$. Higher metallicity is expected to be overestimation, the lower limit is corresponded to the upper limit of the IGM metallicity at $z \sim 2 - 3$ (e.g., D’Odorico et al. 2010).

3. Chemical and spectral evolution

We consider two SFR models with different parameter p_2 : $3 \times 10^4 \text{ Myr } M_\odot^{-1}$ – model A, and $5 \times 10^3 \text{ Myr } M_\odot^{-1}$ – model C. In model A the SFR (absolute) is nearly constant at $\sim 6 M_\odot/\text{yr}$ during first 200 Myr afterwards decreases down to $\sim 0.6 M_\odot/\text{yr}$ at 10 Gyr. The corresponding values of SFR in model C are about 7 times higher, but the timescale, where the rate is constant, is shorter, $\sim 50 \text{ Myr}$. Thus, the rates in both models remain still high at $\sim 5 - 10 \text{ Gyr}$ (redshifts $z \sim 0.5 - 0$) to consider such galaxies as starforming ones (Schiminovich et al. 2007).

Figure 1 presents the galactic spectral luminosity at $t = 7.5 \text{ Gyr}$ (that corresponds the time elapsed from $z = 2$ to 0.2) shown by dash-dotted line (the right axis) and an example of the total spectral distribution (the left axis): the cumulative ionizing background flux (thick grey line) at $z = 0.2$ and distance $d = 100 \text{ kpc}$ from the galaxy. The total spectrum consists of the galactic (dash line) and extragalactic (dotted line) ionizing backgrounds. The strong absorption of the galactic photons within energy range, $E \sim 13.6 - 90 \text{ eV}$, in the galactic disk leads to the control of ionic composition by the extragalactic background. To estimate a significance of the absorption one can see the galactic spectral luminosity (see the right axis). Note that there is a bump around $E \sim 90 - 136 \text{ eV}$, because not all photons emitted by galactic stellar population are absorbed in the disk. Certainly, this is due to our choice of the neutral column densities N_{HI} and N_{HeI} in the disk. In case of the higher column densities the amplitude of the bump decreases. Also the decrease is taken place at large distances from the galaxy, where the extragalactic radiation is dominant. Note that in the range $E \sim 90 - 136 \text{ eV}$ there is the O V ionization potential, $I_{\text{OV}} = 113.9 \text{ eV}$. So that the excess of

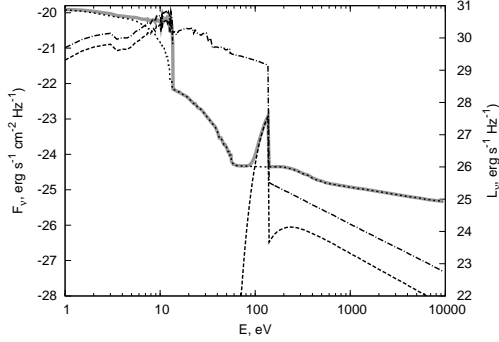


Fig. 1. The cumulative ionizing background flux (thick grey line) at $z = 0.2$ and a distance from the galaxy $d = 100$ kpc, which consists of the UV and X-ray galactic spectrum, attenuated by galactic neutral gas (dash line), the extragalactic ionizing background (dotted line). The galactic spectral luminosity is shown by dash-dotted line (the right axis).

such photons is expected to change the ionization kinetics of oxygen and may lead to higher O VI fraction.

4. The evolution of O VI fraction

Figure 2 shows the evolution of O VI fraction in a gas located at two distances from the galactic center: 70 and 120 kpc. One can see that the O VI fraction is higher 0.1 in a gas with $n \lesssim 2 \times 10^{-4} \text{ cm}^{-3}$ and metallicity $0.1 Z_{\odot}$, the fraction reaches ~ 0.6 at 70 kpc and ~ 0.3 at 120 kpc at $z \lesssim 0.2$. This results in a factor of 2-3 more conservative estimate of the oxygen mass in haloes compared to $M_O = 1.2 \times 10^7 (0.2/f_{\text{OVI}}) M_{\odot}$ (Tumlinson et al. 2011). Thus, the O VI fraction is higher than that in the standard (photo-)equilibrium case, where the maximum O VI fraction is $\sim 0.1 - 0.2$ (e.g., Gnat & Sternberg 2007). Higher O VI fraction obtained in our model leads to more conservative estimate of the oxygen mass in haloes, and consequently weaker constraints on the sources of oxygen.

Note that because of high flux of ionizing radiation at $z \sim 2$ oxygen is mainly locked in the O VII state. The decrease of the ionizing flux with redshift or/and due to decrease of SFR leads to the O VII recombination and growth of the O VI fraction. Actually, after \sim

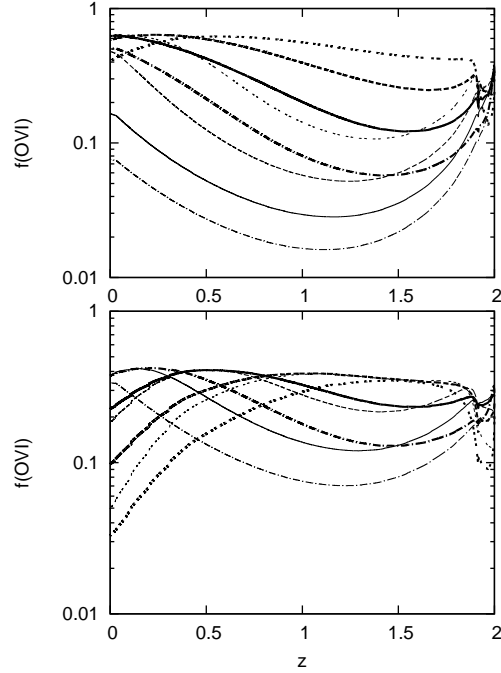


Fig. 2. O VI fraction evolution of gas at distances 70 (upper panel) and 120 kpc (lower panel) from the galactic center for a gas with number density $0.5 \times 10^{-4} \text{ cm}^{-3}$ (dash-dot) 10^{-4} cm^{-3} (solid), $2 \times 10^{-4} \text{ cm}^{-3}$ (dash), $4 \times 10^{-4} \text{ cm}^{-3}$ (dot). Thick and thin lines correspond to isochoric and isobaric models, respectively.

1 – 2 Gyr because the SFR goes down in $\sim 3 - 4$ times compared to the initial value, galactic luminosity decreases, so that the transition from O VII to O VI becomes faster. Under the standard conditions the O VI state is fragile and further recombination leads to lower ionic states. However, the excess of photons with $E > I_{\text{OVI}} = 113.9 \text{ eV}$ emitted by star-forming galaxies does not allow to develop recombination so efficiently: it is almost frozen out at O VI.

5. The O VI column densities

Figure 3 presents the dependence of the O VI column density on the impact parameter assuming 1/10 of solar metallicity gas exposed to the ionizing background evolved as in model C at redshift $z = 0.1$. One

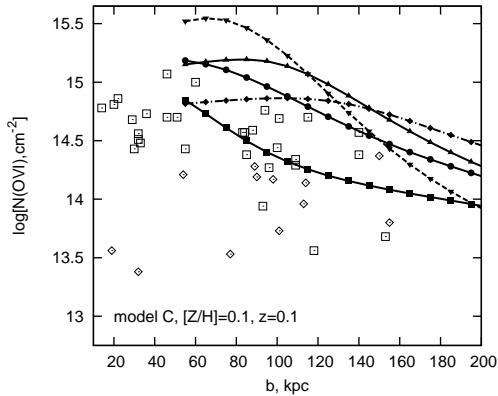


Fig. 3. The dependence of the O VI column density on the impact parameter at redshift $z = 0.1$ and exposed to the galactic background corresponded to the models A and C. The metallicity of gas is $0.1 Z_{\odot}$. Different type of symbols show the column densities for a gas evolved isobarically with number density $0.5 \times 10^{-4} \text{ cm}^{-3}$ (dash-dot line with rombs), 10^{-4} cm^{-3} (solid line with up triangles), $2 \times 10^{-4} \text{ cm}^{-3}$ (dash line with down triangles) and isochorically with $n = 10^{-4} \text{ cm}^{-3}$ (solid line with circles) in the model C, and for a gas evolved isochorically with $n = 10^{-4} \text{ cm}^{-3}$ (solid line with squares) in the model A. The open symbols correspond to the column densities observed in active (squares) and passive (rombs) starforming galaxies (Tumlinson et al. 2011).

can see that the O VI column density ranges in $\log[N(\text{OVI}), \text{cm}^{-2}] \sim 14.3 - 15.3$ at impact parameter $b < 150 \text{ kpc}$ for a gas with $n \lesssim 2 \times 10^{-4} \text{ cm}^{-3}$, that exhibits a good coincidence with the observational data obtained by Tumlinson et al. (2011). The dependence of column density is shallower for lower gas density: one can find a plateau up to $b \lesssim 150 \text{ kpc}$ at $n \lesssim 10^{-4} \text{ cm}^{-3}$.

6. Conclusions

With minimum assumptions we have found physical conditions (density, metallicity of gas, spectrum shape) under which the O VI fraction can reach ~ 0.6 .

Using the PEGASE code we have calculated chemical and spectro-photometric evolution of galaxies, and have chosen two of the models whose sSFR and stellar masses are close to the star-forming galaxies with large O VI column densities (Tumlinson et al. 2011).

We have found that O VI column densities range in $\log[N(\text{OVI}), \text{cm}^{-2}] \sim 14.5 - 15.3$ for $0.1 Z_{\odot}$ gas, and $\sim 12.9 - 14.2$ for $0.01 Z_{\odot}$ gas at impact parameters up to $< 150 \text{ kpc}$. This results in a factor of 2-3 more conservative estimate of the oxygen mass in halos compared to $M_O = 1.2 \times 10^7 (0.2/f_{\text{OVI}}) M_{\odot}$ (Tumlinson et al. 2011).

Acknowledgements. This work is supported by the RFBR through the grants 12-02-00365, 12-02-00917, 12-02-92704, and by Ministry of Education and Science (state contract 2.5641.2011). EV is grateful for support from the "Dynasty" foundation.

References

- Anderson, M.E., & Bregman, J.N. 2010, *ApJ*, 714, 320
- D'Odorico, V., et al. 2010, *MNRAS*, 401, 2715
- Feldmann, R., Hooper, D., Gnedin, N.Y. 2013, *ApJ*, 763, 21
- Ferland G. J., et al. 1998, *PASP*, 110, 761
- Fioc, M., & Rocca-Volmerange, B. 1997, *A&A*, 326, 950
- Gilfanov, M., Grimm, H.-J., Sunyaev, R. 2004, *MNRAS*, 347, L57
- Gnat, O., & Sternberg, A. 2007, *ApJS*, 168, 213
- Haardt, F., & Madau, P. 2001, in *Clusters of Galaxies and the High Redshift Universe Observed in X-rays*, ed. D. M. Neumann & J. T. T. Van, arXiv:astro-ph/0106018
- Hammer, F., et al. 2007, *ApJ*, 662, 322
- Schiminovich, D., et al. 2007, *ApJSS*, 173, 315
- Stanimirović, S., Dickey, J.M., Krćo, M., & Brooks, A.M. 2002, *ApJ*, 576, 773
- Tumlinson, J., et al. 2011, *Science*, 334, 948
- Vasiliev, E. O. 2011, *MNRAS*, 414, 3145